# Using $^{210}Pb$ Simulations for model Comparison and analysing

Marco A Aquino-López[*,†] Nicole K. Sanderson[‡] Maarten Blaauw[§]
J Andrés Christen[¶]

**Abstract**

*Keywords:* Plum, Age-depth models, Chronology, Constant Rate of Supply, Comparison.

[*]Centro de Investigación en Matemáticas (CIMAT), Jalisco s/n, Valenciana, 36023 Guanajuato, GT, Mexico. email: aquino@cimat.mx
[†]Corresponding author.
[‡]College of Life and Environmental Sciences, University of Exeter, Exeter, EX4-4QJ. email: N.K.Sanderson@exeter.ac.uk
[§]School of Natural and Built Environment, Queen's University Belfast, Belfast, BT7-1NN. email:maarten.blaauw@qub.ac.uk
[¶]Centro de Investigación en Matemáticas (CIMAT), Jalisco s/n, Valenciana, 36023 Guanajuato, GT, Mexico. email: jac@cimat.mx

# 1 Introduction

$^{210}Pb$ is radioactive nuclide, which naturally forms in the atmosphere (as well as in the sediment) as result of the decay chain of $^{238}U$. This isotope (with a half-life if 22.23 yr) is commonly used to date recent recent sediments ($<$ 150 to 200 yr). Unlike other dating techniques such as $^{14}C$, a single measurement of $^{210}Pb$ is useless for dating and it is only when a good portion of the decay curve is measured (together with certain assumptions about the sedimentation process) when a chronology can be established. In recent years palaeoecological and pollution studies have gain an increasing interest in the study of recent sediments in order to measure the human impact humans have in the environment. These studies strongly depend on the accuracy of the chronologies in order to correctly assign dates to chemical and biological changes.

The most commonly used model for dating recent sediment using $^{210}Pb$ is the Constant Rate of Supply (CRS) model (Appleby and Oldfield, 1978; Robbins, 1978; Sanchez-Cabeza and Ruiz-Fernández, 2012) also known as Constant Flux - CF model. This is not the only model but it is by far the most popular (see figure 1) and with most flexible assumptions. The CRS model assumes a constant supply of $^{210}Pb$ to the sediment from the atmosphere and allows for changes in the sedimentation rate. In order to estimate a chronology the CRS model uses a ratio between the complete inventory (the complete estimate of the radioactivity in the column of the sediment between the surface and a certain depth where $^{210}Pb$ from the atmosphere can no longer be found) and the remaining inventory from depth $x$ ($t(x) = \frac{1}{\lambda} \log \frac{A_0}{A_x}$, where $A_0$ is the complete inventory, $\lambda$ the decay constant of the $^{210}Pb \approx .03114$).

Other model requiere the assumption of constant supply of $^{210}Pb$ as well as other assumptions of the sedimentation process. The flexibility of the CRS, regarding its assumptions, comes at the cost of the need to measure a good portion of the inventory of the whole core or the use of interpolation in order to fairly estimate the complete inventory of $^{210}Pb$ in the sediment.

This model has received several revisions in order to improve its accuracy and applicability. There are two types of revisions to this model: revisions to its uncertainty (Binford, 1990; Sanchez-Cabeza et al., 2014) and to its applicability when extra information is available -extra dating sources e.g. $^{137}Cs$ or laminated sediments- (Appleby, 1998, 2001, 2008)

A recent study (Barsanti et al., 2020) an inter-laboratory presented a series of data to different laboratories around the world and each laboratory return a chronology.

[Aqui hablar de Bansanti2020]

Recently Aquino-López et al. (2018) presented an alternative to these classical models, by introducing a Bayesian approach to the $^{210}Pb$ dating methodology, called *Plum*. The main idea of this model is to tread every data point as originating from a system which includes the sedimentation process as well as the decay process. This differs from the decay process the CRS model because it uses the decay equation to obtained the age-depth function (which results in a more restrictive age-depth model). *Plum* has shown to provide accurate results with a realistic precision depending on the different case scenarios (Aquino-López et al.,

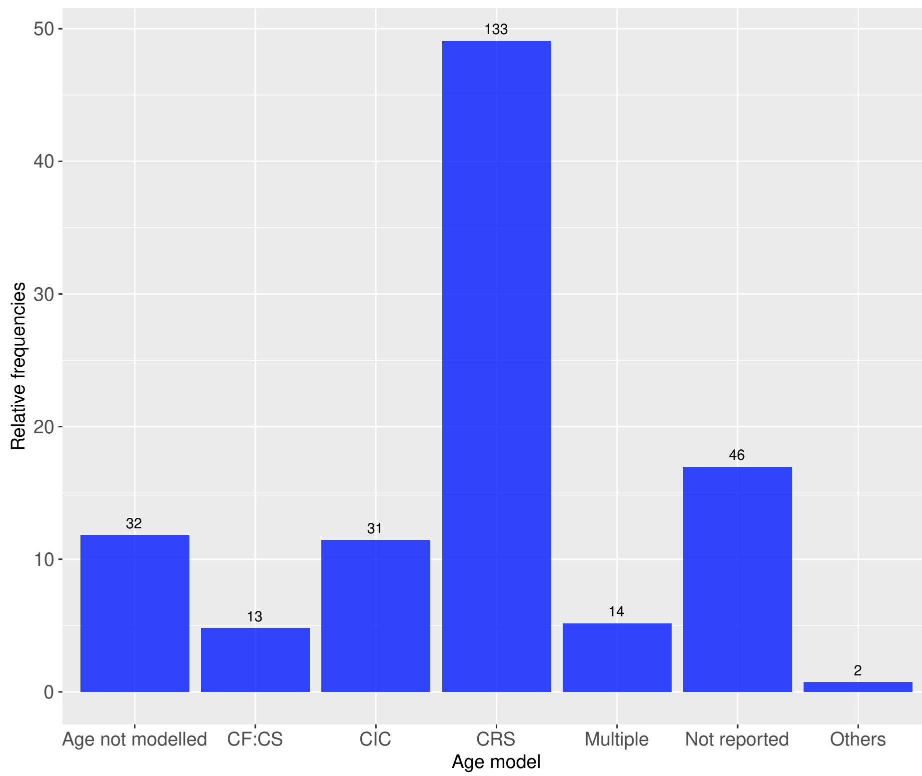


Figure 1: Models used in papers between 1964 and 2017. Data gather by Mustaphi et al. (2019) from literature review of 271 papers. CF:CS model also known as The Constant Flux - Constant Sedimentation (Robbins, 1978), CIC (Constant Initial Concentration) presented by Goldberg (1963); Crozaz et al. (1964); Robbins (1978), CRS - Constant Rate of Supply (Appleby and Oldfield, 1978; Robbins, 1978).

2018, 2020) - both simulations and real cores. Under optimal conditions *Plum* and the CRS model have shown to provide similar results (Aquino-López et al., 2020) with *Plum* providing more realistic uncertainties, with minimal user interaction.

In this study, we tested the CRS model against *Plum* under simulated cores, to which the resulting age-depth model is known, but with the objective to see how different sample size and distribution of the samples affect each model and their resulting chronologies.

[Aqui hablar de Blaauw2019]

# 2 Simulations and Information Percentage

In order to observe the accuracy and precision of any model we need data to which we know the true age-depth function. Blaauw et al. (2018) presented a methodology for simulating radiocarbon dates and as their uncertainty, on the other hand Aquino-López et al. (2018) presented an approach for simulating $^{210}Pb$ data given a age-depth function $f(t)$, it is important to note that this simulations follow the equations presented by Appleby and Oldfield (1978); Robbins (1978). By using the approach presented by Aquino-López et al. (2018) for obtaining $^{210}Pb$ simulated data from and the uncertainty estimations presented by Blaauw et al. (2018), we can obtained resalable $^{210}Pb$ simulated data.

For our simulations we constructed three different scenarios (see table 2), each with their own age-depth functions.

| Label | Age-depth function | $\Phi$ $(\frac{Bq}{m^2yr})$ | Supported $^{210}Pb$ $(\frac{Bq}{kg})$ |
|---|---|---|---|
| Simulation 1 | $\frac{x^2}{4} + \frac{x}{2}$ | 100 | 10 |
| Simulation 2 | $12x - .2x^2$ | 50 | 25 |
| Simulation 3 | $8x + 25\sin(\frac{x}{\pi})$ | 500 | 15 |

Table 1: Simulated age-depth function and parameters used in each simulation

Using the age-depth functions, defined in table 2, we can obtained simulate the activity at any depth or interval (by integrating the curve in such interval).

These concentrations can be interpreted as error-free measurements. Because every equipment is subject to error, we need to replicate this measurement errors. (Blaauw et al., 2018) presents error structure for radiocarbon dates. We can use this structure to our $^{210}Pb$ measurements as both measurements are subject to similar measurement problems.

Let $C_{\hat{x}}$ be the true $^{210}Pb$ concentration in the interval $\hat{x} = [a, b)$, given the age-depth function $t(x)$. To simulate disturbances in the material, we can introduce scatter centred around the true value, $C \sim \mathcal{N}\left(C_{\hat{x}}, x^2_{scat}\right)$, where $x^2_{scat}$ is the amount of scatter for this variable (in this case $x^2_{scat} = 10$). Now, to replicate outliers, we define a shift from the true value ($x_{shift}$), which occurs with a probability $p_{out}$. This results in a new variable $\theta'$ which is defined as

$$\theta' = \begin{cases} \mathcal{U}(\hat{x} - x_{shift}\theta + x_{shift}), & p_{out} \\ \theta, & 1 - p_{out} \end{cases}. \tag{1}$$

To simulate the uncertainty provided by the laboratory, we can define the simulated measurements as $y(\theta') \sim \mathcal{N}\left(\mu(\theta'), \sigma^2\right)$, where $\sigma_R$ is the standard deviation reported by the laboratory. To simulate $\sigma_R$ we use $\sigma_R = \max\left(\sigma_{min}, \mu(\theta')\ \varepsilon\ y_{scat}\ \right)$, where $\sigma_{min}$ is the minimum standard deviation assigned to a measurement. This variable differs between laboratories (we will be using a default value of 1 $Bq/kg$). Finally, $\varepsilon$ is the analytical uncertainty (default .01) and $y_{scat}$ an error multiplier (default 1.5).

For this this study we created a data set for each simulation by integrating in intervals of 1 cm from depth 0 to 30 (where equilibrium was guaranteed).The complete data sets can be found in the Supplementary Material 5 and Figure 2 $^{210}Pb$ concentrations curves.

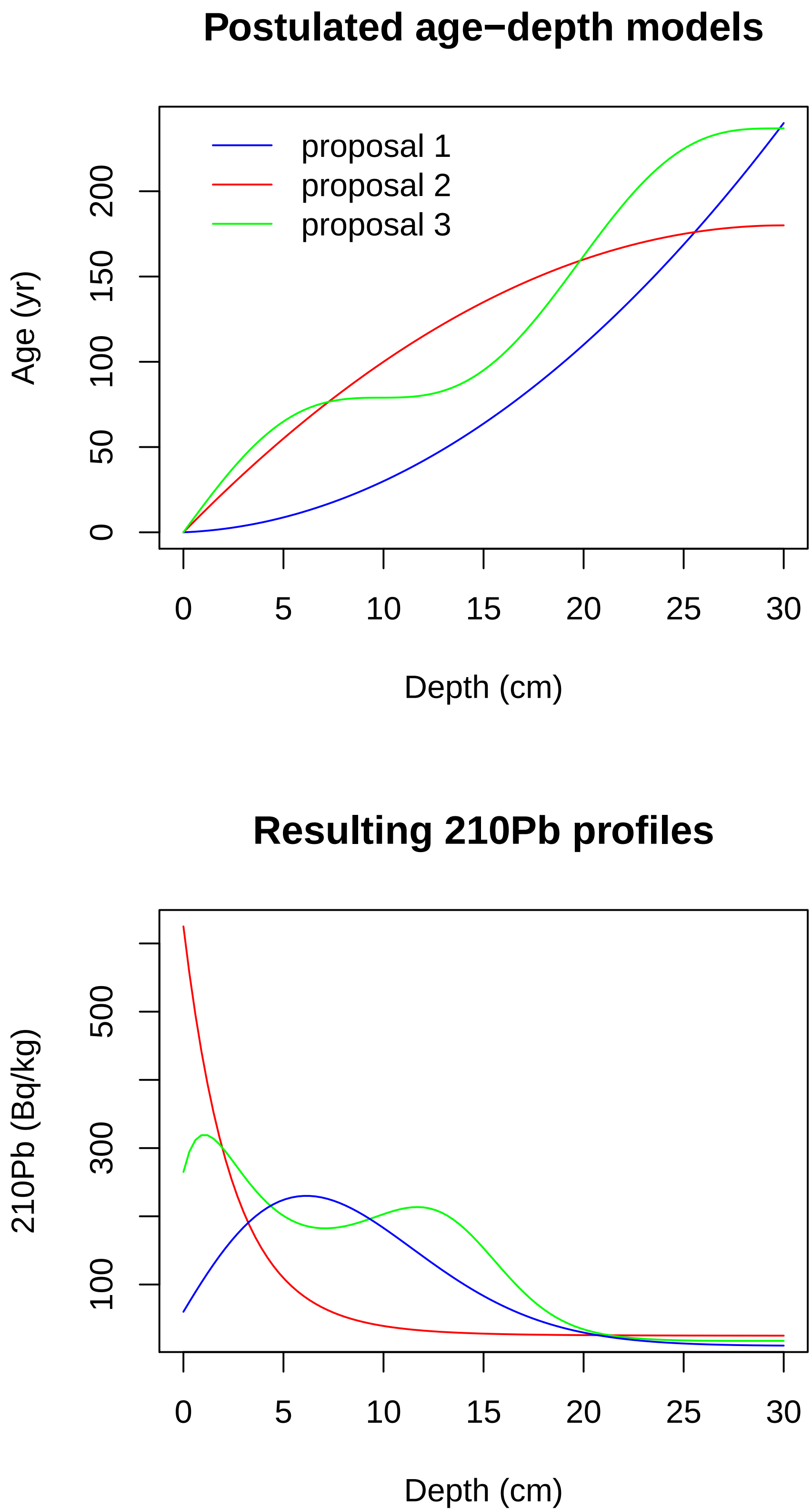




Figure 2: Proposed age-depth functions with their corresponding $^{210}Pb$ profiles. Upper panel: Age-depth function for the three different proposals. Lower panel: Corresponding $^{210}Pb$ profiles in relation to depth.

With these base data sets, we then define a new variable call percentage of information. This variable relates to how many much of the available information was measured. For this we assumed that background was reached at depth $m$, information percentage is define as how much area of the core was measured, e.g. if background was reached at depth 100 cm and the core was sampled very 1 cm if 20 samples are measured, the percentage of information would be 20 %. This variable will help us to have a measuring tool for how many samples are needed for a good chronology without depending on the size of the samples.

## 3 Model Comparison

In order to compare both the CRS and Plum under simular circumstances the previously described data sets will be randomly selected for samples given a information percentage, e.g. for a percentage information of 50% given our 30 sample data set, 14 samples will randomly selected from the samples at depths 1 to 29, and the samples at depth 30 will be always included. This was done to guaranty that background is reached, which is required for the CRS model. In the case of cores which have not reach background, *Plum* (Aquino-López et al., 2018) has shown to provide accurate results without the need of user interference, the CRS can provide a chronology if inventory is completed, which means user innervation. To avoid this problem and to provide a more objective comparison every sampling set will have reach background.

In order to observe different percentage of information affect the accuracy and precision of $^{210}Pb$ models, we used the three simulated data sets created for the previous section. This simulated cores were randomly selected given a percentage of information (e.g. for a 20% information sample, in the 30 cm cores, 6 random samples were selected). Becase the CRS model assumes that background has being reached (In order to reduce user manipulation), we decided to fix the last sample (30 cm depth) for every case, this will facilitate the CRS to provide more accurate results and also gives the model a single last depth to be removed as it is common practice when using this model. 100 individual samples were randomly selected for information percentage from 10% to 100% in a 5% intervals (e.i 10%, 15%, 20%,...,95% and 100%).After a random sample was selected both the CRS model and Plum were performed and compared to the true age value to calculate its accuracy.

In order to observe the precision and accuracy, we decided to calculate the mean of length of the 95% intervals (in yr), the offset (in yr) as well as the normalized accuracy (this variable will show us how far the model is from the true value given its uncertainty).

From Figure 3, we can observe similar results those presented by Blaauw et al. (2018). The classical model (CRS) at first appears to provide a similar result (similar offset) to the Bayesian alternative (*Plum*) with a more precise results (if we only look at the length of the 95% interval). These results can be misleading if we don't analysed the effects of these two parameters in conjunction (offset and length of interval). In order to observe how well the model captures the true ages calculated the normal offset (see Figure 3). These figures shows how on average the models contain the true within their uncertainty intervals (normalized to

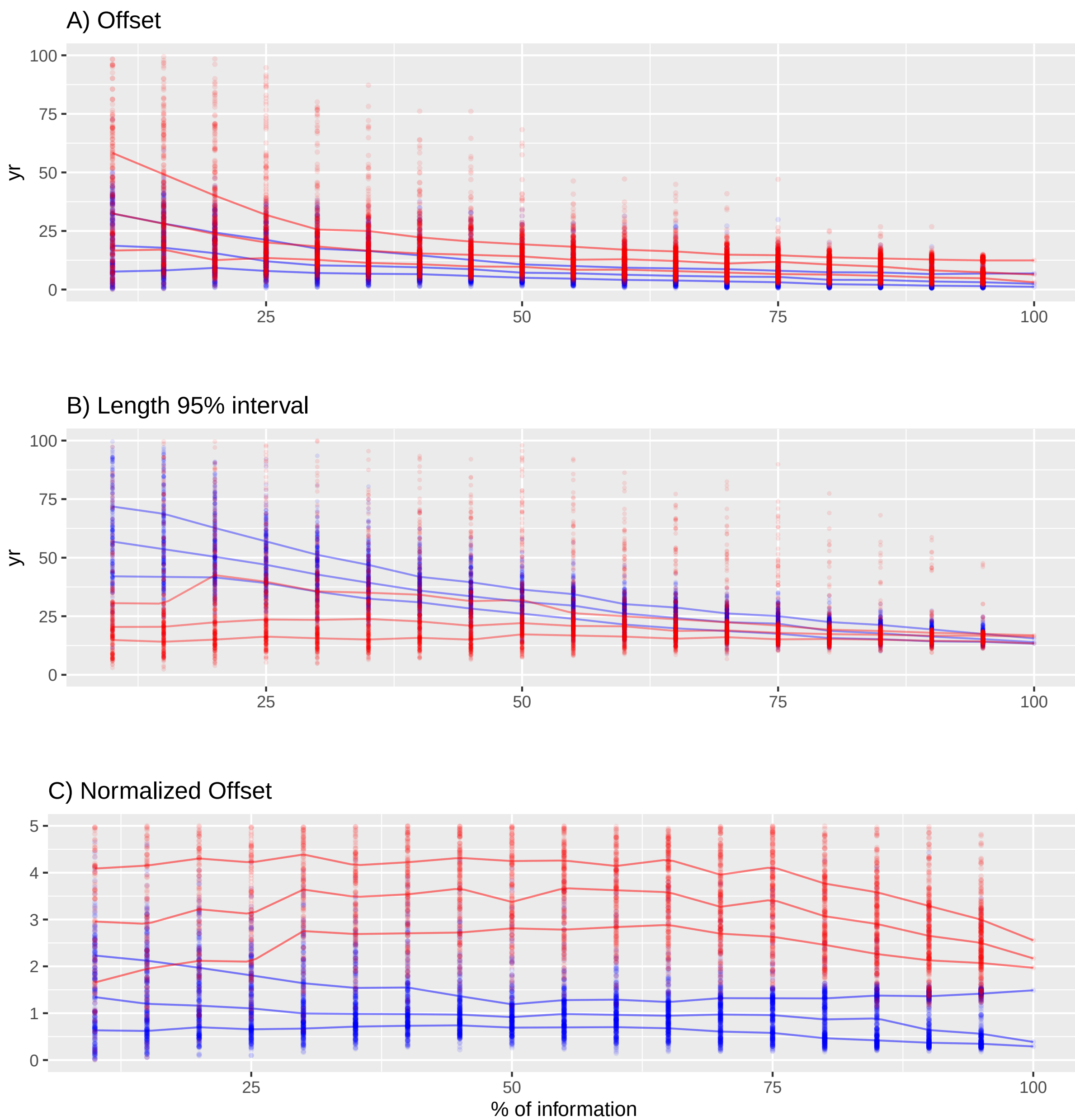


Figure 3: Comparison of the offset (distance between the true age and model), the lenght of the 95% confidence interval (classical) and credible interval (Bayesian) and the Normalized offset between the classical CRS model vs the Bayesian approach *Plum*. Top panel A) shows the offset between the true age and modelled age of the CRS (red) and *Plum* (blue). Middle panel B) length of the 95% confidence interval for the CRS model (in red) and the 95% credible interval of *Plum* (in blue). Bottom panel C) Normalized offset presenting the distance between the modelled age and the true age normalized divided by the standard deviation (in the case of *Plum*, the length of the interval divided by 4), CRS in red and *Plum* in blue.

one standard deviation). Any value which is over the second standard deviations represents that the model is incapable of capturing the true ages within their uncertainty intervals. This means that the CRS provides small uncertainties at the cost of its accuracy. It also appears that the length of the 95% interval and offset is not affected by how much information is provided to the model. This is a results of the use of interpolation used by the method.

On the other hand, *Plum*, which is a Bayesian method, shows more accurate results as more information is given to the model, this are similart to the ones found by Blaauw et al. (2018). When we observe the regular offset (not normalized), we observed that Plum provides a smaller offset in comparison to the CRS model, this in combination with slightly bigger uncertainties results on a consistently accurate model which is capable of capturing the true values within its uncertainty intervals. This result supports the clame that *Plum* provides more realistic uncertainties when compared to the CRS.

Plum has 87.86% (4686/5333) of its runs under the 2 standard deviations, on the other hand the CRS model only has 7.48% (399/5333) and only .54% (29/5333) lies under the 1 standard deviation which is the most commonly reported interval when reporting CRS results. We can also observe a clear structure on the way Plum increases its accuracy and precision to obtained a better chronology, on the side the CRS model appears to not have this structure.

Figure 5 shows the normalized accuracy of every simulation by depth, similar the results presented above, we observe how the information percentage is irrelevant to the accuracy of the CRS model, contrary to the results obtained by *Plum* which accuracy is increased by the available information.

# 4 Conclusions and Discussion

These results show a clear bias provided by the CRS model. Aquino-López et al. (2018) discussed this point and states that the bias is the product of the use of a logarithmic function for the age-depth function. It is also evident from these results that the CRS model's uncertainties are not sufficient to capture the true age-depth function. This is an important point given the fact that is common practice amount the $^{210}Pb$ dating community to report credible intervals to one single deviation (instad of the 95% confidence intervals). Other confidence intervals have being proposed for this method (Sanchez-Cabeza et al., 2014) but the fact that this intervals are even smaller than the ones obtained by error propagation (Appleby, 2001) is of consent.

Previous work on model comparison (Barsanti et al., 2020) have shown the problems with the variability of $^{210}Pb$ results even when different users apply the same or similar models to a single set of data. In this work, on the other hard reduced user input and try to show the effects of different samples takes from the same dataset. The results of this experiment showed that the CRS model can provide extremely different results even when the data originates from the same data set. Figure 4 showed that the CRS model appears to dont learn from using more data. This is explains why over the years, many authors have insisted in

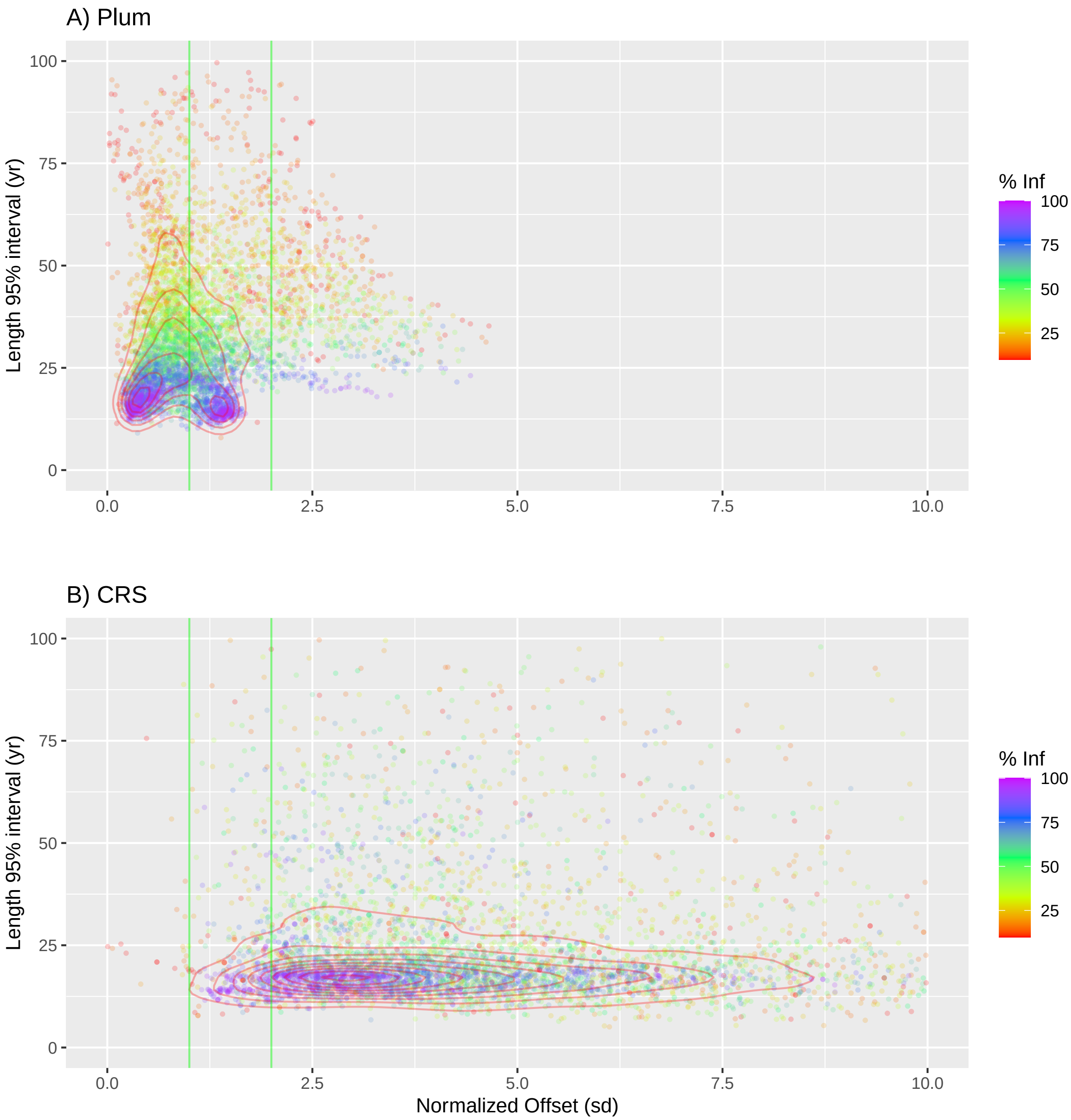
A) Plum
Length 95% interval (yr)
100
75
50
25
0
0.0
2.5
5.0
7.5
10.0
% Inf
100
75
50
25
B) CRS
Length 95% interval (yr)
100
75
50
25
0
0.0
2.5
5.0
7.5
10.0
Normalized Offset (sd)
% Inf
100
75
50
25

Figure 4:

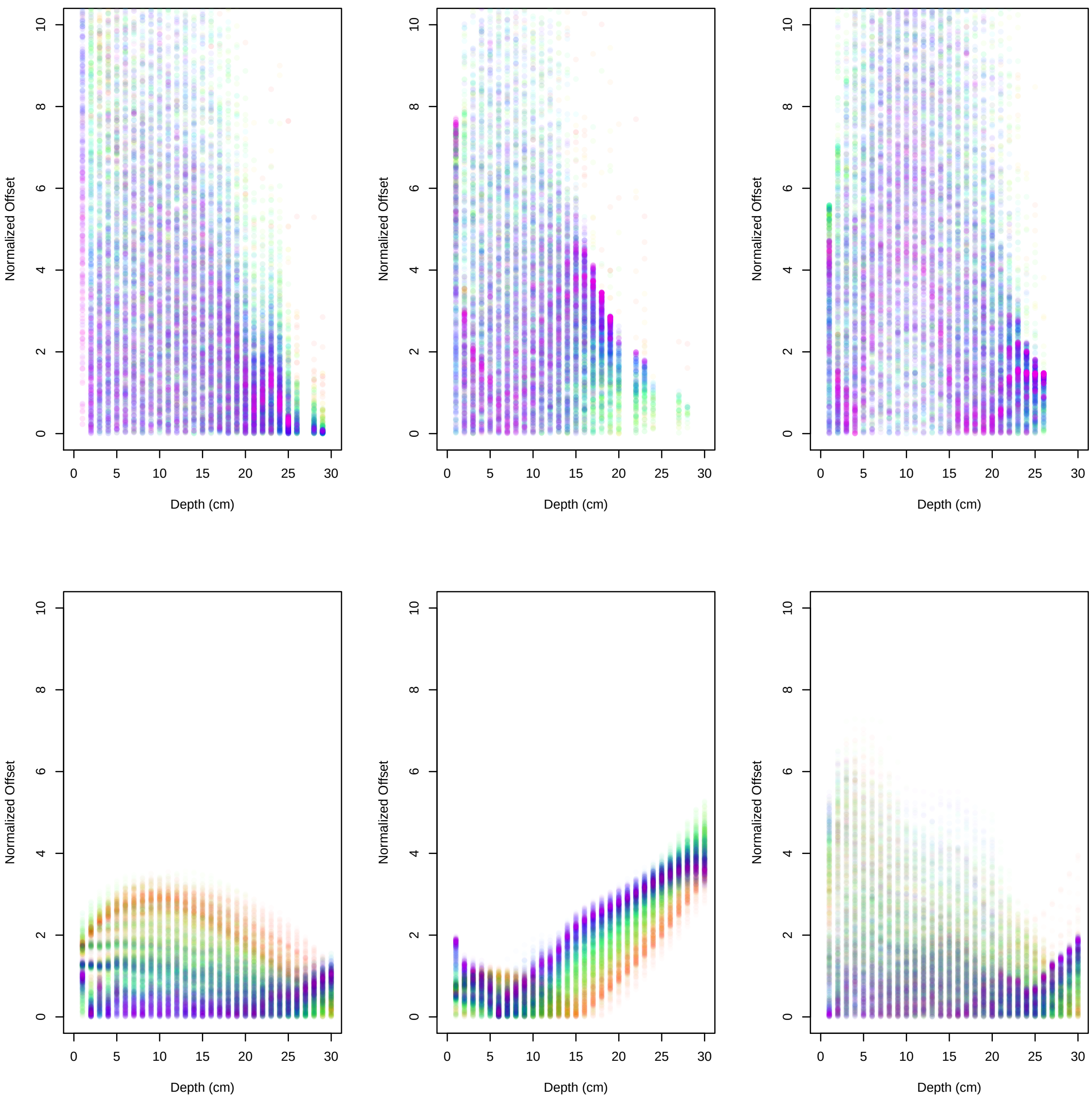


Figure 5: Normalized accuracy of every simulation

the use of other dating techniques to validate the chronology provided by the CRS (Sanchez-Cabeza and Ruiz-Fernández, 2012; Barsanti et al., 2020; Aquino-López et al., 2020). These results highly encourage the need of validating the CRS chronology before its use.

On the other hand, *Plum* shows a consistent accurate result by capturing the true values within the 95% credible intervals on a more constant matter. It is important to note that one of the big advantages of *Plum* is its increasing accuracy and precision reduction as more data becomes available.

These results show the mean accuracy and precision throughout the whole chronology, this means that the problems of increased accumulation rate provided by the logarithmic function in the CRS function may be a result of the consistently big offset provided by the CRS model. Some CRS users agree that the results from this model should be discarded after a certain age limit

# References


Appleby, P. (2008). Three decades of dating recent sediments by fallout radionuclides: a review. *The Holocene*, 18(1):83–93.

Appleby, P. and Oldfield, F. (1978). The calculation of lead-210 dates assuming a constant rate of supply of unsupported 210pb to the sediment. *Catena*, 5(1):1–8.

Appleby, P. G. (1998). Dating recent sediments by Pb-210: Problems and solutions. *Proc. 2nd NKS/EKO-1 Seminar, Helsinki, 2-4 April 1997, STUK, Helsinki*, pages 7–24.

Appleby, P. G. (2001). Chronostratigraphic techniques in recent sediments. *Tracking Environmental Change Using Lake Sediments: Basin Analysis, Coring, and Chronological Techniques*, pages "171–203".

Aquino-López, M. A., Blaauw, M., Christen, J. A., and Sanderson, N. K. (2018). Bayesian analysis of 210pb dating. *Journal of Agricultural, Biological and Environmental Statistics*, 23(3):317–333.

Aquino-López, M. A., Ruiz-Fernández, A. C., Blaauw, M., and Sanchez-Cabeza, J.-A. (2020). Comparing classical and bayesian 210pb dating models in human-impacted aquatic environments. *Quaternary Geochronology*, 60:101106.

Barsanti, M., Garcia-Tenorio, R., Schirone, A., Rozmaric, M., Ruiz-Fernández, A., Sanchez-Cabeza, J., Delbono, I., Conte, F., Godoy, J. D. O., Heijnis, H., Eriksson, M., Hatje, V., Laissaoui, A., Nguyen, H., Okuku, E., Al-Rousan, S. A., Uddin, S., Yii, M., and Osvath, I. (2020). Challenges and limitations of the 210pb sediment dating method: Results from an IAEA modelling interlaboratory comparison exercise. *Quaternary Geochronology*, 59:101093.

Binford, M. W. (1990). Calculation and uncertainty analysis of $^{210}Pb$ dates for PIRLA project lake sediment cores. *Journal of Paleolimnology*, 3:253–267.

Blaauw, M., Christen, J. A., Bennett, K., and Reimer, P. J. (2018). Double the dates and go for Bayes — impacts of model choice, dating density and quality on chronologies. *Quaternary Science Reviews*, 188:58–66.

Crozaz, G., Picciotto, E., and de Breuck, W. (1964). Antarctic snow chronology with pb210. *Journal of Geophysical Research*, 69(12):2597–2604.

Goldberg, E. D. (1963). Geochronology with pb-210. *Radioactive Dating*, pages 121–131.

Mustaphi, C. J. C., Brahney, J., Aquino-López, M. A., Goring, S., Orton, K., Noronha, A., Czaplewski, J., Asena, Q., Paton, S., and Brushworth, J. P. (2019). Guidelines for reporting and archiving 210pb sediment chronologies to improve fidelity and extend data lifecycle. *Quaternary Geochronology*, 52:77–87.

Robbins, J. (1978). Geochemical and geophysical applications of radioactive lead. *The biogeochemistry of lead in the environment*, pages 285–393.

Sanchez-Cabeza, J. A. and Ruiz-Fernández, A. C. (2012). 210Pb sediment radiochronology: An integrated formulation and classification of dating models. *Geochimica et Cosmochimica Acta*, 82:183–200.

Sanchez-Cabeza, J. A., Ruiz-Fernández, A. C., Ontiveros-Cuadras, J. F., Pérez Bernal, L. H., and Olid, C. (2014). Monte Carlo uncertainty calculation of 210Pb chronologies and accumulation rates of sediments and peat bogs. *Quaternary Geochronology*, 23:80–93.

# 5 Supplementary Material

Data for each simulation is hosted at (add github here)

| Label | Depth (cm) | Density ($g/cm^3$) | 210Pb (Bq/kg) | sd(210Pb) | Thickness (cm) | 226Ra (Bq/kg) | sd(226Ra) |
|---|---|---|---|---|---|---|---|
| Sim01-01 | 1 | 0.10009 | 63.50103 | 2.85755 | 1 | 23.8045 | 1.125 |
| Sim01-02 | 2 | 0.10064 | 80.08738 | 3.60393 | 1 | 23.2924 | 1.125 |
| Sim01-03 | 3 | 0.10173 | 98.32806 | 4.42476 | 1 | 23.434 | 1.125 |
| Sim01-04 | 4 | 0.10334 | 125.45705 | 5.64557 | 1 | 26.0873 | 1.125 |
| Sim01-05 | 5 | 0.10547 | 141.27971 | 6.35759 | 1 | 22.8041 | 1.125 |
| Sim01-06 | 6 | 0.10809 | 130.27571 | 5.86241 | 1 | 23.4333 | 1.125 |
| Sim01-07 | 7 | 0.11116 | 134.04051 | 6.03182 | 1 | 25.6156 | 1.125 |
| Sim01-08 | 8 | 0.11466 | 129.69245 | 5.83616 | 1 | 26.1371 | 1.125 |
| Sim01-09 | 9 | 0.11855 | 134.93655 | 6.07214 | 1 | 25.4813 | 1.125 |
| Sim01-10 | 10 | 0.12278 | 109.39886 | 4.92295 | 1 | 25.8877 | 1.125 |
| Sim01-11 | 11 | 0.12731 | 110.68133 | 4.98066 | 1 | 24.4414 | 1.125 |
| Sim01-12 | 12 | 0.13209 | 102.38094 | 4.60714 | 1 | 24.9053 | 1.125 |
| Sim01-13 | 13 | 0.13706 | 75.80895 | 3.4114 | 1 | 22.9151 | 1.125 |
| Sim01-14 | 14 | 0.14218 | 77.60406 | 3.49218 | 1 | 24.4808 | 1.125 |
| Sim01-15 | 15 | 0.14738 | 68.4401 | 3.0798 | 1 | 24.9343 | 1.125 |
| Sim01-16 | 16 | 0.15262 | 60.72037 | 2.73242 | 1 | 25.2659 | 1.125 |
| Sim01-17 | 17 | 0.15782 | 50.28147 | 2.26267 | 1 | 22.961 | 1.125 |
| Sim01-18 | 18 | 0.16294 | 44.24641 | 1.99109 | 1 | 22.9139 | 1.125 |
| Sim01-19 | 19 | 0.16791 | 39.85997 | 1.7937 | 1 | 28.3774 | 1.125 |
| Sim01-20 | 20 | 0.17269 | 38.40823 | 1.72837 | 1 | 23.5379 | 1.125 |
| Sim01-21 | 21 | 0.17722 | 32.75922 | 1.47416 | 1 | 25.4363 | 1.125 |
| Sim01-22 | 22 | 0.18145 | 28.02545 | 1.26115 | 1 | 24.8995 | 1.125 |
| Sim01-23 | 23 | 0.18534 | 27.8749 | 1.25437 | 1 | 22.6783 | 1.125 |
| Sim01-24 | 24 | 0.18884 | 30.74797 | 1.38366 | 1 | 24.8575 | 1.125 |
| Sim01-25 | 25 | 0.19191 | 28.36187 | 1.27628 | 1 | 24.8724 | 1.125 |
| Sim01-26 | 26 | 0.19453 | 27.24535 | 1.22604 | 1 | 24.3778 | 1.125 |
| Sim01-27 | 27 | 0.19666 | 23.59236 | 1.06166 | 1 | 24.7209 | 1.125 |
| Sim01-28 | 28 | 0.19827 | 25.74855 | 1.15868 | 1 | 24.6615 | 1.125 |
| Sim01-29 | 29 | 0.19936 | 25.05368 | 1.12742 | 1 | 24.7199 | 1.125 |
| Sim01-30 | 30 | 0.19991 | 25.0065 | 1.12529 | 1 | 24.4937 | 1.125 |

| Label | Depth (cm) | Density ($g/cm^3$) | 210Pb (Bq/kg) | sd(210Pb) | Thickness (cm) | 226Ra (Bq/kg) | sd(226Ra) |
|---|---|---|---|---|---|---|---|
| Sim02-01 | 1 | 0.1001 | 909.3928 | 40.9227 | 1 | 8.9761 | 0.45 |
| Sim02-02 | 2 | 0.1006 | 683.9989 | 30.7799 | 1 | 10.0607 | 0.45 |
| Sim02-03 | 3 | 0.1017 | 453.0503 | 20.3873 | 1 | 9.8701 | 0.45 |
| Sim02-04 | 4 | 0.1033 | 310.7897 | 13.9855 | 1 | 10.37 | 0.45 |
| Sim02-05 | 5 | 0.1055 | 218.0058 | 9.8103 | 1 | 10.0418 | 0.45 |
| Sim02-06 | 6 | 0.1081 | 158.6974 | 7.1414 | 1 | 10.104 | 0.45 |
| Sim02-07 | 7 | 0.1112 | 113.9062 | 5.1258 | 1 | 10.2049 | 0.45 |
| Sim02-08 | 8 | 0.1147 | 75.5493 | 3.3997 | 1 | 9.334 | 0.45 |
| Sim02-09 | 9 | 0.1185 | 56.6252 | 2.5481 | 1 | 10.5145 | 0.45 |
| Sim02-10 | 10 | 0.1228 | 44.1595 | 1.9872 | 1 | 9.8677 | 0.45 |
| Sim02-11 | 11 | 0.1273 | 34.7448 | 1.5635 | 1 | 9.7694 | 0.45 |
| Sim02-12 | 12 | 0.1321 | 25.384 | 1.1423 | 1 | 10.5134 | 0.45 |
| Sim02-13 | 13 | 0.1371 | 24.0007 | 1.08 | 1 | 10.4589 | 0.45 |
| Sim02-14 | 14 | 0.1422 | 21.3643 | 1 | 1 | 9.9504 | 0.45 |
| Sim02-15 | 15 | 0.1474 | 17.7932 | 1 | 1 | 10.5135 | 0.45 |
| Sim02-16 | 16 | 0.1526 | 15.0416 | 1 | 1 | 10.3362 | 0.45 |
| Sim02-17 | 17 | 0.1578 | 14.2937 | 1 | 1 | 10.5131 | 0.45 |
| Sim02-18 | 18 | 0.1629 | 12.3844 | 1 | 1 | 10.368 | 0.45 |
| Sim02-19 | 19 | 0.1679 | 12.6023 | 1 | 1 | 10.5297 | 0.45 |
| Sim02-20 | 20 | 0.1727 | 11.9329 | 1 | 1 | 10.0924 | 0.45 |
| Sim02-21 | 21 | 0.1772 | 9.301 | 1 | 1 | 10.118 | 0.45 |
| Sim02-22 | 22 | 0.1815 | 10.7777 | 1 | 1 | 10.249 | 0.45 |
| Sim02-23 | 23 | 0.1853 | 12.9491 | 1 | 1 | 10.134 | 0.45 |
| Sim02-24 | 24 | 0.1888 | 10.6571 | 1 | 1 | 10.1151 | 0.45 |
| Sim02-25 | 25 | 0.1919 | 9.6297 | 1 | 1 | 9.6608 | 0.45 |
| Sim02-26 | 26 | 0.1945 | 8.4331 | 1 | 1 | 8.7821 | 0.45 |
| Sim02-27 | 27 | 0.1967 | 10.4921 | 1 | 1 | 9.8995 | 0.45 |
| Sim02-28 | 28 | 0.1983 | 11.135 | 1 | 1 | 9.2481 | 0.45 |
| Sim02-29 | 29 | 0.1994 | 10.109 | 1 | 1 | 10.4398 | 0.45 |
| Sim02-30 | 30 | 0.1999 | 9.5404 | 1 | 1 | 10.1114 | 0.45 |

| Label | Depth (cm) | Density ($g/cm^3$) | 210Pb (Bq/kg) | sd(210Pb) | Thickness (cm) | 226Ra (Bq/kg) | sd(226Ra) |
|---|---|---|---|---|---|---|---|
| Sim03-01 | 1 | 0.1001 | 6384.1354 | 287.2861 | 1 | 15.8007 | 0.675 |
| Sim03-02 | 2 | 0.1006 | 3550.0809 | 159.7536 | 1 | 14.5245 | 0.675 |
| Sim03-03 | 3 | 0.1017 | 1954.5702 | 87.9557 | 1 | 15.6527 | 0.675 |
| Sim03-04 | 4 | 0.1033 | 1183.8917 | 53.2751 | 1 | 14.5175 | 0.675 |
| Sim03-05 | 5 | 0.1055 | 760.2132 | 34.2096 | 1 | 14.9242 | 0.675 |
| Sim03-06 | 6 | 0.1081 | 360.2553 | 16.2115 | 1 | 14.801 | 0.675 |
| Sim03-07 | 7 | 0.1112 | 212.9402 | 9.5823 | 1 | 14.8738 | 0.675 |
| Sim03-08 | 8 | 0.1147 | 104.2684 | 4.6921 | 1 | 14.9028 | 0.675 |
| Sim03-09 | 9 | 0.1185 | 44.3849 | 1.9973 | 1 | 15.0768 | 0.675 |
| Sim03-10 | 10 | 0.1228 | 18.6447 | 1 | 1 | 15.3764 | 0.675 |
| Sim03-11 | 11 | 0.1273 | 23.2778 | 1.0475 | 1 | 14.6231 | 0.675 |
| Sim03-12 | 12 | 0.1321 | 53.1587 | 2.3921 | 1 | 15.1629 | 0.675 |
| Sim03-13 | 13 | 0.1371 | 97.363 | 4.3813 | 1 | 14.3047 | 0.675 |
| Sim03-14 | 14 | 0.1422 | 116.9788 | 5.264 | 1 | 14.0261 | 0.675 |
| Sim03-15 | 15 | 0.1474 | 153.2901 | 6.8981 | 1 | 15.9723 | 0.675 |
| Sim03-16 | 16 | 0.1526 | 151.8496 | 6.8332 | 1 | 14.7579 | 0.675 |
| Sim03-17 | 17 | 0.1578 | 136.3609 | 6.1362 | 1 | 16.114 | 0.675 |
| Sim03-18 | 18 | 0.1629 | 107.2736 | 4.8273 | 1 | 15.4595 | 0.675 |
| Sim03-19 | 19 | 0.1679 | 76.8966 | 3.4603 | 1 | 15.9439 | 0.675 |
| Sim03-20 | 20 | 0.1727 | 48.9213 | 2.2015 | 1 | 14.6235 | 0.675 |
| Sim03-21 | 21 | 0.1772 | 40.4439 | 1.82 | 1 | 14.6716 | 0.675 |
| Sim03-22 | 22 | 0.1815 | 26.5638 | 1.1954 | 1 | 16.2541 | 0.675 |
| Sim03-23 | 23 | 0.1853 | 21.714 | 1 | 1 | 14.4826 | 0.675 |
| Sim03-24 | 24 | 0.1888 | 17.6428 | 1 | 1 | 15.5109 | 0.675 |
| Sim03-25 | 25 | 0.1919 | 17.3533 | 1 | 1 | 13.6898 | 0.675 |
| Sim03-26 | 26 | 0.1945 | 17.4211 | 1 | 1 | 14.4684 | 0.675 |
| Sim03-27 | 27 | 0.1967 | 16.4246 | 1 | 1 | 15.3889 | 0.675 |
| Sim03-28 | 28 | 0.1983 | 12.4828 | 1 | 1 | 15.0698 | 0.675 |
| Sim03-29 | 29 | 0.1994 | 13.5514 | 1 | 1 | 15.2346 | 0.675 |
| Sim03-30 | 30 | 0.1999 | 14.3145 | 1 | 1 | 14.7846 | 0.675 |